JOURNAL OF NEUROCHEMISTRY | 2008 | 104 | 1020–1031 doi: 10.1111/j.1471-4159.2007.05034.x

The C-terminus of the metabotropic glutamate receptor 1b regulates dimerization of the receptor

Rosaria Remelli,* Melanie J. Robbins† and R. A. Jeffrey McIlhinney*

*Medical Research Council Anatomical Neuropharmacology Unit, Oxford, UK

†Neurophysiology and Pharmacology, Psychiatry CEDD, GlaxoSmithKline Pharmaceuticals, Harlow, Essex, UK

Abstract

The Group C G protein-coupled receptors include the metabotropic glutamate receptors (mGluRs), the $GABA_B$ receptor, the calcium sensor and several taste receptors, most of which are obligate dimers, indeed recent work has shown that dimerization is necessary for the activation of these receptors. Consequently factors that regulate their ability to homo- or heterodimerize are important. The Group 1 mGluRs include mGluR1 and mGluR5 both of which have splice variants with altered C-termini. In this study, we show that mGluR1b is a dimer and that it does not efficiently heterodimerize with mGluR1a, unlike the two splice variants of mGluR5 that can heterodimerize. Mutation of a positively charged motif (RRKK) at the C-terminus of the mGluR1b tail permits mGluR1b to heterodimerize with mGluR1a. Co-expression of mGluR1a and mGluR1b in COS-7 cells results in the accumulation of mGluR1b in intracellular inclusions that do not contain mGluR1a. This behaviour is mimicked by a chimera of the lymphocyte antigen CD2 with the C-terminus of mGluR1b (pCD1b) and depends on the presence of the RRKK motif. These accumulations are immunoreactive for endoplasmic reticulum (ER) markers, but not Golgi and ERGIC markers. This segregation of mGluR1b from other ER proteins may contribute to its failure to dimerize with mGluR1a.

Keywords: C-terminus, dimerization, endoplasmic reticulum, metabotropic glutamate receptor 1b, retention, trafficking.

J. Neurochem. (2008) **104**, 1020–1031.

The major excitatory neurotransmitters in the mammalian CNS are aspartic and glutamic acid (Mayer and Westbrook 1987; Hollmann and Heinemann 1994). These act through glutamate receptors and play an important role in many physiological functions, ranging from development, to learning and memory (Malenka and Nicoll 1993). Glutamate receptors can be subdivided into two groups, those forming ion channels, namely the AMPA, kainate and NMDA receptors, and those acting through the heterotrimeric G proteins, termed the metabotropic glutamate receptors (mGluRs). There are eight members of the latter family that can be further subdivided into three subgroups, on the basis of their sequence homology, agonist specificity and signal transduction pathway, and within these mGluR1 and mGluR5 form Group 1. Both mGluR1 and mGluR5 have quisqualate as their most potent agonist, couple to $G_{q/11}$ activating phospholipase C, and have different splice variants, resulting in alterations in their C-terminal sequences. The alternative splicing of mGluR1 results in the removal of 318 amino acids from the C-terminus of mGluR1a and the addition of 22–26 residues to form mGluR1b, c, d, e and f. A similar splice site is present in mGluR5 where the insertion of 32 amino acids 49 residues after the last transmembrane region of mGluR5a gives rise to mGluR5b (Tanabe *et al.* 1992; Pin and Duvoisin 1995; Conn and Pin 1997).

All of the mGluRs fall into the Group C class of G protein-coupled receptors which also include the $GABA_B$ receptor, the calcium sensing receptor, the retinoic acid inducible genes, and some of the taste and pheromone receptors (Robbins *et al.* 2000; Pin *et al.* 2004). These have in common a heptahelical domain and a large extracellular domain which for most of them forms a disulphide bonded

Received July 4, 2007; revised manuscript received September 4, 2007; accepted September 26, 2007.

Address correspondence and reprint requests to Dr R. A. Jeffrey McIlhinney, MRC Anatomical Neuropharmacology Unit, Mansfield Road, Oxford OX1 3TH, UK. E-mail: jeff.mcilhinney@pharm.ox.ac.uk

Abbreviations used: CFP, cyan fluorescent protein; EndoH, endoglycosidase H; ER, endoplasmic reticulum; FRET, fluorescence resonance energy transfer; HA, haemagglutinin antigen; HBSS, Hank's Balanced Salt Solution; HEK, human embryonic kidney cells; mGluR, metabotropic glutamate receptor; PBS, phosphate-buffered saline; PDI, protein disulphide isomerase; ROI, region of interest; SDS–PAGE, sodium dodecyl sulphate–polyacrylamide gel electrophoresis; YFP, yellow fluorescent protein.

dimer (Romano *et al.* 1996; Tsuji *et al.* 2000; Pin and Acher 2002). Biochemical and structural studies have shown that each of these extracellular regions forms a Venus Flytrap domain between which there are direct interactions (Kunishima *et al.* 2000; Tsuji *et al.* 2000; Liu *et al.* 2004a). From structural and functional studies, it has become apparent that agonist binding causes a change in the relative orientation of the Venus Flytrap domains which results in the activation of these receptors (Kunishima *et al.* 2000; Bessis *et al.* 2002; Tsuchiya *et al.* 2002; Kniazeff *et al.* 2004a,b). Consequently, the dimerization of these receptors is important for their function and for most of these receptors this seems to be driven by their extracellular domains and takes place in the endoplasmic reticulum (ER) (Ray *et al.* 1999; Robbins *et al.* 1999; Ray and Hauschild 2000; Romano *et al.* 2001; Liu *et al.* 2004a; Villemure *et al.* 2005). Indeed, soluble domains of the extracellular domains of mGluR1 and mGluR4 are secreted as dimers (Han and Hampson 1999; Robbins *et al.* 1999; Kunishima *et al.* 2000; Selkirk *et al.* 2002) although the cysteine that forms the disulphide bridge between the extracellular domains is not essential for dimer formation, nor for functioning of the receptor (Tsuji *et al.* 2000; Romano *et al.* 2001). With the exception of the reported heterodimerization of the mGluR1 and calcium sensing receptor, there has been no evidence for the heterodimerization of other mGluRs, in fact mGluR1 and mGluR5 do not form heterodimers when co-expressed in cells (Romano *et al.* 1996; Robbins *et al.* 1999; Gama *et al.* 2001). However, given that mGluR1a and mGluR1b are identical at their N-terminus and that this is the region that drives the dimerization of the receptors, it was a surprise to discover that these two subtypes of mGluR1 did not heterodimerize when co-expressed in human embryonic kidney (HEK) 293 cells (Robbins *et al.* 1999).

We have previously shown that an RRKK motif at the C-terminus of mGluR1b can cause its retention in the ER but that, on mutation of this to AAAA, the receptor can traffic normally to the cell surface (Chan *et al.* 2001). This result, together with our observation of the lack of heterodimerization between mGluR1a and mGluR1b, led us to speculate that the RRKK motif in mGluR1b might regulate its dimerization with other mGluR1 isoforms. Therefore we have studied the dimerization and trafficking of mGluR1b, and mutants thereof, in transfected cells. In this study, we provide the first direct evidence that mGluR1b is a dimer and show that the RRKK motif prevents it from efficiently dimerizing with other forms of mGluR1. Consistent with this, in rat cerebellum, where both mGluR1a and mGluR1b are co-expressed in Purkinje cells, co-immunoprecipitation experiments did not reveal heterodimerization of the two isoforms of the receptor. Immunocytochemical studies with cell compartment specific antibodies showed that mGluR1b, and a chimaeric molecule containing its C-terminus, is apparently segregated from other membrane proteins in the ER and this may contribute to its failure to dimerize with other mGluR1 splice variants.

Materials and methods

Materials

Protein *N*-glycosidase F (pNGaseF) and Endoglycosidase H (EndoH) were purchased from Roche Biochemicals (Lewes, UK), and Lipofectamine 2000 from Invitrogen (Carlsbad, CA, USA). JetPEI was supplied by Autogen Bioclear (Colne, UK). Horseradish peroxidase-conjugated anti-mouse and rabbit antibodies were purchased from Promega (Southampton, UK) and the Talon resin was from BD Biosciences (San Diego, CA, USA). Antibodies used in this study were rabbit anti-GluR1a C- and N-terminal and a rabbit anti-mGluR1b C-terminal antibody that have been described previously (Ciruela *et al.* 1999a; Chan *et al.* 2001), an anti-myc mouse monoclonal antibody clone 9E10 produced in house from a hybridoma, a rabbit anti-haemagglutinin antigen (HA) (BAbCO, Berkeley, CA, USA), rabbit anti-sec24 a gift from Dr David Stephens (University of Bristol, Bristol, UK), mouse anti-GM130 (BD Biosciences, Oxford, UK), mouse anti-protein disulphide isomerase (PDI; Stressgen, San Diego, CA, USA), mouse anti-ERGIC 53 (Alexis Biochemicals, San Diego, CA, USA), a mouse monoclonal anti-CD2 a gift from Dr Neil Barclay (Oxford, UK), Alexa 568-coupled goat anti-rabbit, Alexa 488-coupled goat anti-rabbit, Alexa 488-coupled goat anti-mouse and Alexa 568-coupled goat anti-mouse (Molecular Probes, Eugene, OR, USA).

Methods

Recombinant constructs

N-terminally FLAG-tagged mGluR1a, mGluR1b and their mutants have been described previously (Ciruela *et al.* 1999b; Chan *et al.* 2001). A *Bgl*II/*Xho*I digest was performed on pcDNA3-myc-HisA (Invitrogen) and the vector gel purified. The C-terminal tail of mGluR1b was amplified by PCR using the primers 5′-GGC-AGCAAGAAGAAGATCTGCACCCGG-3′ and 5′-GCAGTGTGG-GGGTTTCTCGAGCTGCGCATGTGC-3′ and the product digested with *Bgl*II/*Xho*I and ligated into the pcDNA3 myc-HisA vector to give pcDNA3myc-His-1. The mGluR1b, in a pcDNA3 vector (Ciruela *et al.* 1999a), was digested with *Bgl*II and the N-terminal region isolated as the smaller fragment. This was then ligated into the *Bgl*II digested, calf intestinal alkaline phosphatase treated pcDNA3myc-His-1 to yield the final mGluR1b-mycHis tagged at the C-terminus. Exactly the same steps, except using mGluRMM18 as the substrate in the PCR reaction, yielded mGluRMM18-mycHis. To produce the yellow fluorescent (YFP) and cyan fluorescent (CFP) protein forms of mGluR1b and mGluRMM18, the plasmids encoding the myc-His versions of the proteins were digested with *Bam*HI and *Xho*I to excise the entire cDNA fragment of each, and these ligated into *Bgl*II *Xho*I digested pEYFP-N1 and pECFP-N1 vectors (Clontech, Mountain View, CA, USA).

The mGluR5a and mGluR5b cDNAs and their C-terminally HA-tagged versions in pcDNA3 were gifts from Dr Francesco Ferraguti and Dr Corrado Corti and have been described previously (Mion *et al.* 2001). Both mGluR5a and 5b-mycHis versions were prepared by amplifying the C-terminal of mGluR5-HA in pcDNA3 from

beyond an *Eco*R47III site to the stop codon with the primers 5′-CGCAGGATGCACAGCAACAGGT-3′ and 5′-CAGTTCTAG-ACAACGATGAAGA-3′. The PCR product and the mGluR5 in pcDNA3 were digested with *Eco*R47III and *Xba*I and ligated to produce an mGluR5 without a stop codon and with an *Xba*I site at the C-terminus. The whole sequence was then removed from the pcDNA3 using *Eco*RI and *Xba*I and ligated into pcDNA3-mycHis to give mGluR5a or 5b-mycHis.

The production of the constructs pCD1b and pCDMM18, containing the C-termini of mGluR1b and mGluRMM18, respectively, fused with the N-terminus and transmembrane domain of the lymphocyte antigen CD2 has been described previously (Chan *et al.* 2001). To produce CD2-YFP the plasmid containing CD2 fused to the C-terminal tail of mGluR1a previously described (Chan *et al.* 2001) was digested with *Bam*HI and *Not*I to remove the mGluR1a sequence. YFP (pEYFP-N1; Clontech) was amplified by PCR with the primers 5′-GACTCAGATCTCGAGCTAAGCTTCGAATTC-3′ and 5′-GATCTAGAGTCGCGGCCGCTTTACTTGTAC-3′ containing 5′ *Bgl*II and 3′ *Not*I sites. The PCR product was gel purified, digested with the appropriate enzymes, and ligated into the digested CD2 plasmid to generate the construct CD2-YFP. For all constructs the sequence changes were confirmed by DNA sequencing.

Tissue culture

Human embryonic kidney 293 cells and COS-7 cells were grown in Dulbecco's Modified Eagle's Medium (Sigma Chemical Co., Poole, UK) supplemented with 10% (v/v) foetal calf serum (Invitrogen), 2 mmol/L L-glutamine, 50 U/mL penicillin, 50 μg/mL streptomycin (all from Invitrogen) at 37°C, in a humidified atmosphere of 5% CO_2. For microscopy the cells were plated onto glass coverslips. Cells were either transfected using a calcium phosphate protocol or jetPEI, a polyethylenimine-derived transfection reagent (Qbiogene, Cambridge, UK). The calcium phosphate method was adapted from (Jordan *et al.* 1996). The transfection mixture consists of: 540 μL sterile water, 10 μg DNA, 186 μL of 1 mol/L $CaCl_2$ and 750 μL of 2× HEPES-buffered saline pH 7.2. The mixture was gently mixed and left for 45 s to allow the formation of the precipitate. An appropriate volume was added directly to the cells (750 μL for a 25-cm^2 flask, 200 μL for a well of a 6-well plate). JetPEI was used according to the manufacturer's instructions. For transient transfections with cDNAs encoding mGluR5, the medium was replaced with glutamate-free medium [Glutamax Dulbecco's Modified Eagle's Medium, 10% (v/v) dialysed foetal calf serum] at 6 or 24 h after transfection, to avoid agonist-induced degradation of the receptor.

Endoglycosidase treatment and SDS–PAGE analysis

Membranes prepared from cells transfected with the proteins of interest were digested with pNGaseF or EndoH as described earlier. Samples were prepared for polyacrylamide gel electrophoresis (PAGE) by heating at 60°C for 15 min in 62.5 mmol/L Tris–HCl pH 6.6 containing 1% sodium dodecyl sulphate (SDS), 0.01% bromophenol blue, 20 mmol/L dithiothreitol and 10% glycerol (SDS sample buffer). The proteins separated by SDS–PAGE were transferred to a polyvinylidene difluoride membrane using a BioRad Transblot semi-dry transfer system (BioRad, Hemel Hempstead, UK) and immunoblotted as described previously (Ciruela *et al.* 1999b, 2000).

Membrane preparation and immunoprecipitation

Membranes were prepared from transfected cells and rat cerebellum as described by (Chan *et al.* 2001). For the immunoprecipitation from rat cerebellum, synaptic plasma membranes were solubilized at 20°C for 10 min, in 50 mmol/L Tris–HCl (pH 7.2) containing 0.1 mol/L NaCl (Tris–saline), 1% SDS and protease inhibitors, with a protein : detergent ratio of 1 : 5. The supernatant was diluted 1 : 10 with 1% Triton X-100 in Tris–saline and centrifuged at 100 000 g_{av} for 1 h at 4°C. The supernatant was removed and the mGluR1a receptor was incubated with rabbit-anti-mGluR1a antibody (5 μg) overnight at 4°C, and the immunocomplexes isolated by adding protein G Sepharose, 50 μL of a 1 : 1 aqueous suspension. After rotation for 2 h at 4°C, the Sepharose beads were exhaustively washed and the bound proteins eluted by incubation with SDS sample buffer.

To investigate the dimerization of mGluRs, a modification of the co-immunoprecipitation was performed as follows: cell membranes were prepared 48 h after transfection of HEK293 cells with the two proteins, one of which was myc-His tagged. The membranes were solubilized in Tris–saline containing 1% SDS, in order to disrupt completely any weak non-covalent interactions. The sample was then diluted 1 : 10 in Tris–saline containing 1% Triton X-100, imidazole added to 2.5 mmol/L, and centrifuged at 15 000 g_{av} for 15 min, at 4°C. The supernatant was rotated for 1 h with 50 μL Talon resin (Clontech), which strongly binds to the His tag. After extensive washing with 1% Triton X-100 in Tris–saline containing 2.5 mmol/L imidazole, the proteins were eluted with a small volume of Tris–saline containing 1% Triton X-100 and 0.25 mol/L imidazole. As a negative control, the precipitation of the FLAG-tagged receptor was performed in parallel omitting the myc-His-tagged receptor. The eluate was heated at 60°C for 30 min after the addition of SDS sample buffer. The eluted proteins were then analysed by SDS–PAGE and immunoblotting, together with a fraction of the supernatant, as a control for the input material.

Immunocytochemistry

Cells to be processed were cultured on 22-mm diameter borosilicate glass coverslips in a six-well plate and transfected as appropriate. At 48 h post-transfection, the medium was aspirated and the cells carefully washed in phosphate-buffered saline (PBS) and fixed with 4% (w/v) *p*-formaldehyde in PBS for 5 min at 20°C. The fixed cells were washed in Tris–saline, pH 7.4 for 5 min, and where necessary, permeabilized with 0.25% Triton X-100 for 5 min at 20°C. After incubation in blocking buffer [1% (w/v) bovine serum albumin and 1% (v/v) normal goat serum in PBS] for 30 min, each coverslip was overlaid with 150 μL of primary antibody appropriately diluted in blocking buffer and incubated for at least 1 h at 20°C in a moist chamber. After three washes in blocking buffer, the coverslips were incubated with a 1/1000 dilution of the appropriate fluorophore-conjugated secondary antibody for 1 h at 20°C. The coverslips were then washed three times in PBS and mounted on microscope slides in Vectashield mounting medium (Vector Laboratories, Peterborough, UK) and sealed with clear nail varnish. The images were taken using Zeiss LSM510 confocal scanning microscope mounted on an Axiovert 100M inverted

microscope (Carl Zeiss Ltd, Welwyn Garden City, UK). Antibodies were used at the following dilutions rabbit anti-HA 1/1000, mouse anti-myc 1/10, rabbit anti-sec24 1/100, mouse anti-ERGIC 53 1/100, rabbit anti-PDI 1/400, rabbit anti-GM130 1/400, rabbit anti-mGluR1a C-terminus 1/300, rabbit anti-mGluR1a N-terminus 1/100, rabbit anti-mGluR1b C-terminus 1/300 and mouse anti-CD2 1/20.

Calcium imaging

Human embryonic kidney cells 293, 24 h after transfection with the different mGluR constructs or a control plasmid (pcDNA3), were subcultured onto poly-D-lysine coated coverslips and incubated with glutamate-free medium for a further 24 h. The cells were washed twice with HEPES-buffered Hank's Balanced Salt Solution containing 2 mmol/L $CaCl_2$ (HBSS), and then incubated at 20°C in 1 mL HBSS containing 1 μmol/L Fluo-4 (Molecular Probes) and 0.03% pluronic F-127 (Invitrogen) for 1 h. After three 5 min washes with HBSS the cells were imaged on a Zeiss LSM510 confocal scanning microscope, using the 20× lens of the Axiovert 100M inverted microscope. Images were scanned every 2 s using a 488 nm excitation and 530–550 nm emission filters. After monitoring the cells for 2 min, glutamate at 20 μmol/L was used to stimulate the cells. The cell responses were quantified using the Zeiss LSM software and the results plotted as a ratio of the Fluorescence emission (F) divided by the initial unstimulated fluorescence (F_0). For the control samples transfected with pcDNA3 0.5% Triton X-100 was added at the indicated time to show that these cells had loaded with Fluo-4. Data were collected from a minimum of 14 cells and the results analysed in GraphPad Prism (GraphPad Software, San Diego, CA, USA) using the Kruskal–Wallis method for analysis of variance.

FRET analysis

The fluorescence resonance energy transfer (FRET) occurring between the mGluRMM18 or mGluR1b-YFP and mGluRMM18 or mGluR1b-CFP subunits was determined using acceptor photobleaching (Nashmi *et al.* 2003; Liu *et al.* 2004b). Cells were transfected with equal amounts of the YFP and CFP mGluR1 constructs, and after 48 h, imaged on a Zeiss LSM510 scanning confocal microscope, using a 40× oil immersion lens. The YFP and CFP were excited using the 514 and 458 nm lines of the He–Ne laser and the bleaching of the YFP carried out by repetitive scanning (30 iterations) of the region of interest (ROI) on the cells using 90% of full laser power at 514 nm. The YFP emission was collected through a long pass LP530 nm filter and the CFP fluorescence through a band pass filter BP480–520 nm. ROI were defined in the ER of the cells, taking care to avoid large intracellular inclusions, using a pinhole of 206 μm. After taking five 1 s scans across the cell, the ROI was bleached and five additional scans were collected. The FRET signal was calculated as the fractional increase in the CFP fluorescence signal in the ROI after the bleach thus: $[(CFP_{post\text{-}bleach} - CFP_{pre\text{-}bleach})/CFP_{post\text{-}bleach}] \times 100$, after correction for the background signal, and the weak increase in CFP fluorescence seen after the photobleaching protocol. Data was collected from a minimum of 30 cells and the results analysed in GraphPad using the Kruskal–Wallis method for ANOVA.

Results

Characterization of the mGluR1b-mycHis constructs

In our previous studies we used antibodies to the C-terminal region of mGluR1a to perform immunoprecipitations form cells labelled with ^{35}S-methionine (Robbins *et al.* 1999). In order to allow for more stringent solubilization conditions prior to affinity-isolation of the receptors, we prepared C-terminally myc-His-tagged version of mGluR1b and its mutant form in which the RRKK motif was changed to AAAA (mGluRMM18). These were examined for their expression in transfected COS-7 cells and cell surface expression by immunofluorescence. This showed that the mGluRMM18-mycHis was present at the cell surface, giving a granular pattern of staining, whilst the mGluR1b-mycHis construct gave a much weaker granular pattern of immunoreactivity (Fig. 1a). Immunostaining of permeabilized cells expressing these constructs showed that both were present in the cells at comparable levels and that the mGluR1b-mycHis formed intracellular inclusions that were not present in the mGluRMM18-mycHis cells (see also Fig. 5). Endoglycosidase treatment of the constructs expressed in HEK293 cells showed that the mGluR1b-mycHis was fully EndoH sensitive indicating that it was predominantly retained in the ER. In contrast, the mGluRMM18-mycHis-tagged receptor was EndoH resistant, consistent with our previously reported findings on mGluR1b (Chan *et al.* 2001) (Fig. 1b). It should be noted that that the dimer and monomer bands for the glycosylated forms of mGluRMM18-mycHis appear to migrate more slowly than those formed by mGluR1b-mycHis indicating that the former is more fully glycosylated. The totally de-glycosylated pNGaseF digested protein core of the two proteins is, as expected, the same size. It should be noted that the apparently SDS-resistant dimers of the short splice variants of mGluR1, present in these SDS-denaturing gels have been reported elsewhere and are formed during the processing of the samples (Mary *et al.* 1998; Mateos *et al.* 1998; Chan *et al.* 2001; Francesconi and Duvoisin 2002).

All of the mGluR1b constructs gave a similar peak calcium response following challenge with 20 μmol/L glutamate, indicating that they were functionally coupled (Fig 1c). The mGluRMM18-mycHis receptor calcium response appears to be more prolonged than that of either mGluR1b or mGluR1b-mycHis, and this may reflect its greater cell surface expression. The peak response evoked by mGluR1b was not significantly different from that of mGluRMM18, despite the fact that the wild type has a much lower surface expression compared with the mutant. This suggests that a small number of functional receptors on the cell surface are sufficient to induce a maximal response, which might be limited by other factors such as G protein availability. Therefore, the elevated surface expression of

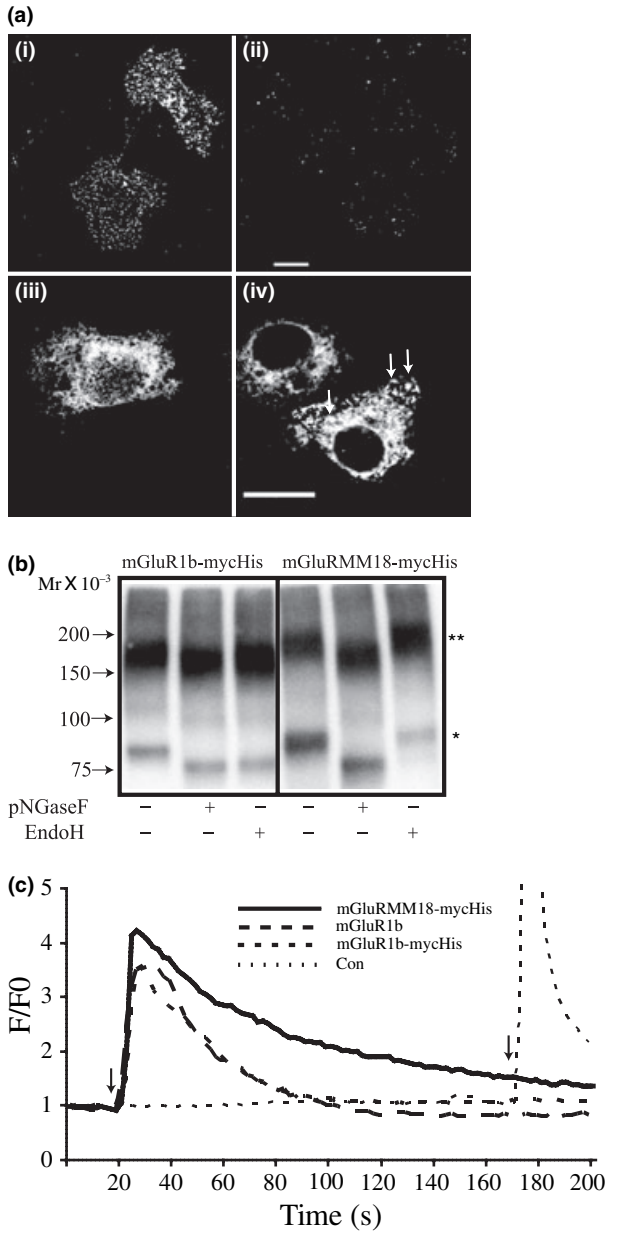

Fig. 1 (a) Immunofluorescence of mGluR1b-mycHis and mGluRMM18-mycHis in COS-7 cells. COS-7 cells were transfected with either mGluR1b-mycHis [a(ii and iv)] or mGluRMM18-mycHis [a(i and iii)]. After 48 h the cells were fixed and immunostained for the receptor using a rabbit N-terminal anti-mGluR1b antibody. In panels [a(iii and iv)], the cells were treated with 0.25% Triton X-100 prior to the primary antibody incubation to permeabilize the cells. The scale bar is 10 μm and the arrows show the inclusions formed by the mGluR1b-mycHis. (b) Endoglycosidase treatment of membranes from HEK293 cells expressing either mGluR1b-mycHis or mGluRMM18-mycHis. Membranes were prepared from the cells 48 h after transfection and treated with the indicated endoglycosidases. After SDS–PAGE and western blotting the receptors were detected using an anti-myc antibody. The mGluR1b shows almost complete EndoH sensitivity, as indicated by its reduction in size, whereas the mGluRMM18-mycHis is almost completely EndoH resistant. The position of the molecular weight markers are indicated by the arrows and the position of the monomer and dimer forms of mGluR1b are indicated by the single and double asterisks respectively. Similar results were obtained in three separate experiments. (c) Calcium responses evoked by stimulating mGluR1b, mGluR1b-mycHis and mGluRMM18-mycHis. HEK293 cells were transfected with the indicated constructs and after 48 h their calcium responses to 20 μmol/L glutamate determined using the calcium sensitive dye, Fluo-4. The time of addition of the glutamate, or 0.5% Triton X-100 to the control cells, is indicated by the arrow. All of the mGluR1b constructs gave a response to glutamate with no significant difference in the mean peak responses (mGluR1b 3.55 ± 0.31, mGluR1b-mycHis 3.6 ± 0.35 and mGluRMM18-mycHis 4.1 ± 0.38). The results are the mean ± SEM responses from 14, 16 and 21 cells respectively. However, the area under the curve for the mGluRMM18-mycHis responses was significantly different from that of the mGluR1b and mGluR1b-mycHis ($p < 0.05$), and these were not different from each other. Similar results were obtained in two separate experiments.

mGluRMM18 would only increase the receptor reserve, without altering the maximal response.

Dimerization of mGluR1b with itself and mGluR1a

As the mGluRs form disulphide bonded dimers, SDS-solubilization will not disrupt them, but will guarantee the disassociation of non-covalent or inadvertent associations caused by the solubilization. In order to maximize recovery of the target proteins during their subsequent affinity isolation, the SDS-solubilized samples were diluted into 1% Triton X-100 to reduce the SDS concentration to 0.1%, prior to the isolation step. Thus using the myc-His-tagged constructs, affinity-isolations were performed, using Talon resin, from SDS-solubilized cell membranes to test if the homodimerization of mGluR1b with itself and heterodimerization with mGluRMM18 could be detected. As can be seen in Fig. 2a, co-expression of mGluR1b-mycHis and FLAG-tagged mGluR1b and immunoprecipitation of the mGluR1b-mycHis, resulted in the co-immunoprecipitation of FLAG-tagged mGluR1b, indicating that mGluR1b can form homodimers of these constructs in the cells. However, if FLAG-tagged mGluR1b and mGluRMM18-mycHis were co-expressed together then we consistently failed to co-immunoprecipitate the two proteins, suggesting that they do not heterodimerize to a significant extent under these conditions (Fig. 2a).

Having established that the Talon resin could be used to demonstrate the dimerization of mGluR1b, the dimerization of mGluR1a and mGluR1b was examined using co-expression of both mGluR1b-mycHis and mGluRMM18-mycHis with FLAG-tagged-mGluR1a. As can be seen in Fig. 2b, mGluR1a is only weakly co-immunoprecipitated with mGluR1b-mycHis, but significantly more of it is brought down when it is co-expressed with mGluRMM18-mycHis. In

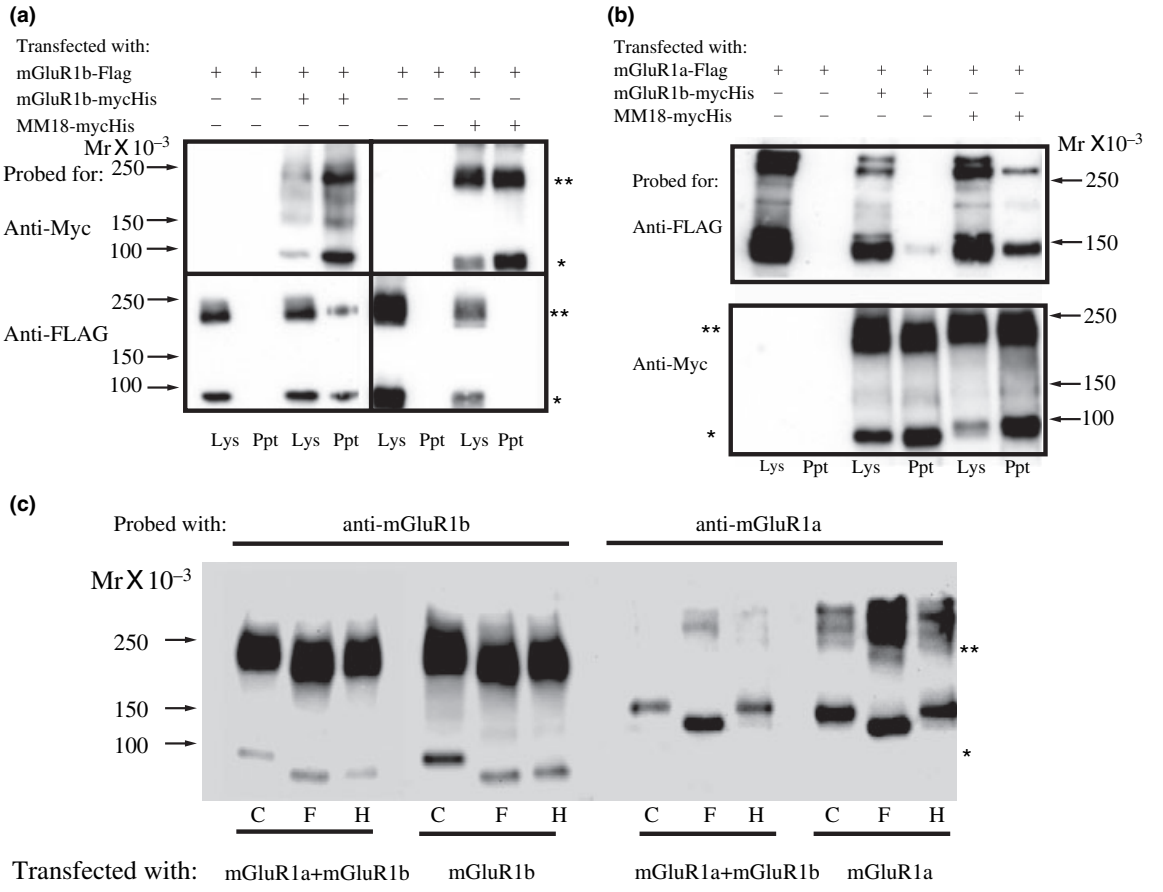

Fig. 2 (a) Talon isolation of FLAG-tagged mGluR1b, by mGluR1b-mycHis or mGluRMM18-mycHis, from SDS-solubilized cell membranes from cells transfected with the indicated cDNAs. HEK293 cells were transfected as shown and after 48 h cell membranes were prepared from the cells. The solubilized material was incubated with Talon resin to isolate the (His)6 form of the receptor and the isolate analysed on SDS–polyacrylamide gels followed by western blotting for the indicated epitope tag. The starting material is indicated by Lys and the Talon isolate by Ppt. Note that whilst mGluR1b and mGluRMM18 form homodimers they do not heterodimerize as shown by the absence of a Talon isolated FLAG-tagged band in the lane where both FLAG-tagged mGluR1b and mGluRMM18-mycHis are co-expressed. Similar results were obtained in three separate experiments. (b) Talon isolation of FLAG-tagged mGluR1a, by mGluR1b-mycHis and mGluRMM18-mycHis, from SDS-solubilized cell membranes from cells transfected with the indicated cDNAs. Note the relatively weak co-isolation of FLAG-tagged mGluR1a with mGluR1b-mycHis compared with when FLAG-tagged mGluR1a is co-expressed with mGluRMM18-mycHis. Similar results were obtained in three separate experiments and in two further experiments no co-immunoprecipitation of mGluR1a with mGluR1b was seen. (c) Endoglycosidase sensitivity of mGluR1b and mGluR1a when expressed alone or together. HEK293 cells were transfected with the indicated cDNAs and after 48 h membranes were prepared from the cells. These were subjected to treatment with no enzyme (C) or with EndoH (H) or pNGaseF (F). The digests were analysed on 5% SDS–polyacrylamide gels followed by immunoblotting for the different receptors. The endoglycosidase sensitivity of both mGluR1a and mGluR1b is not altered when they are co-expressed, suggesting that they do not associate and are not trafficking together to the cell surface. In all the panels, the position of the molecular weight markers are indicated by the arrows and the position of the monomer and dimer forms of mGluR1b are indicated by the single and double asterisks respectively. Similar results were obtained in two separate experiments.

three experiments results similar to those shown here were obtained, in two more we failed to co-immunoprecipitate mGluR1a and mGluR1b suggesting that the two mGluR1 subtypes are only weakly associated. If mGluR1b and mGluR1a were to heterodimerize then we reasoned that either the mGluR1a would act as a chaperone for mGluR1b causing it to move to the cell surface and become EndoH resistant or the mGluR1a associated with mGluR1b would be ER retained and become EndoH sensitive. Therefore, we examined the endoglycosidase sensitivity of the two receptor isoforms after their co-expression in HEK293 cells. In this experiment, the glycosylation status of both mGluR1a and 1b was unchanged when they are co-expressed, suggesting that they do not associate to any significant extent, consistent with the co-immunoprecipitation experiments (Fig. 2c).

To further examine the possibility that mGluR1b or mGluRMM18 were dimerizing, a FRET analysis was performed to see whether the C-termini of the different

receptors when expressed as YFP/CFP C-terminally tagged pairs, were in proximity. The FRET signal was determined by photobleaching the YFP versions of the proteins and monitoring the increase in the CFP fluorescence in their CFP forms, because of the acceptor YFP being bleached. The results showed a mean fluorescence increase for mGluR1b-YFP/CFP pair of 9.9% ± 3.9 (SD; 32 cells), with the mGluRMM18-YFP/CFP pair giving 9.7% ± 3.5 (SD; 35) FRET. The mGluRMM18-YFP/mGluR1b-CFP pair however only gave a 3.2% ± 3.4 (SD; 35) FRET signal. The FRET values obtained from mGluRMM18-YFP/CFP pair, and the mGluR1b-YFP/CFP pair, were not significantly different, but both were significantly different from the mGluRMM18-YFP and mGluR1b-CFP pair ($p > 0.01$). Although the FRET signals are low they are comparable with those reported for similar C-terminal truncated constructs of mGluR1a (Tateyama *et al.* 2004). These data are also consistent with the mGluR1b and mGluRMM18 forming dimers, whereas the mGluRMM18/mGluR1b pair do not.

This prompted us to ask if the alternative splice variants of the other Group 1 mGluRs, namely mGluR5a and 5b, were able to heterodimerize, or whether their alternatively spliced C-termini also prevented heterodimerization. Therefore, mGluR5a and 5b carrying different epitope tags were co-expressed in HEK293 cells and immunoprecipitated separately. The results show clearly that the two mGluR5 splice variants do indeed heterodimerize (Fig. 3).

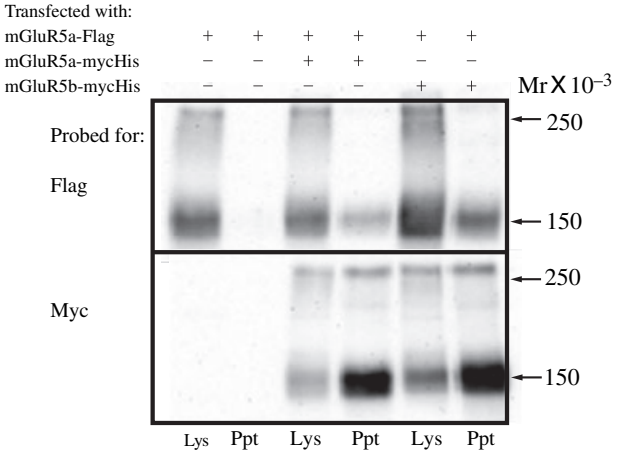

Fig. 3 Talon isolation of FLAG-tagged mGluR5a, by mGluR5a-mycHis or mGluR5b-mycHis, from SDS-solubilized cell membranes from cells transfected with the indicated cDNAs. HEK293 cells were transfected as shown and after 48 h cell membranes were prepared from the cells. The solubilized material was incubated with Talon resin to isolate the (His)6 form of the receptor and the isolate analysed on SDS–polyacrylamide gels followed by western blotting for the indicated epitope tag. The starting material is indicated by Lys and the Talon isolate by Ppt. The position of the molecular weight markers are indicated by the arrows. Similar results were obtained in three separate experiments.

mGluR1a and mGluR1b do not dimerize in the rat cerebellum

Together these data show that the affinity isolation method described here can demonstrate the dimerization of the different mGluRs and provides convincing evidence that the RRKK motif in the C-terminus of mGluR1b is involved in the prevention of heterodimerization of mGluR1b with mGluR1a and can also prevent the association of mGluR1b with its mutated form mGluRMM18-mycHis.

It remains possible that, in the brain, where the mGluR1b receptor is fully glycosylated (Chan *et al.* 2001), mGluR1a could act as a chaperone for mGluR1b, especially in the cerebellum where the two splice variants are co-expressed in Purkinje cells (Mateos *et al.* 2000). Therefore, we solubilized cerebellar membranes from rat brains using SDS and immunoprecipitated mGluR1a using a C-terminal antibody. The resulting immunoprecipitate was split into two aliquots and each immunoblotted for either mGluR1a or mGluR1b. The results show that whilst we obtained good solubilization of the mGluRs and recovered the mGluR1a in good yield, we could not detect mGluR1b in these precipitates (Fig. 4). The same results were obtained in two separate experiments. Thus in cerebellar synaptic membranes, mGluR1a and mGluR1b are not associated in heterodimers.

The ER retention motif causes segregation of mGluR1a and mGluR1b and causes the latter to form intracellular ER-derived accumulations

As mGluR1b does not heterodimerize with mGluRMM18 or mGluR1a we examined the intracellular distribution of mGluR1a, when co-expressed with either mGluR1b or mGluRMM18 in COS-7 cells. The results shown in Fig. 5

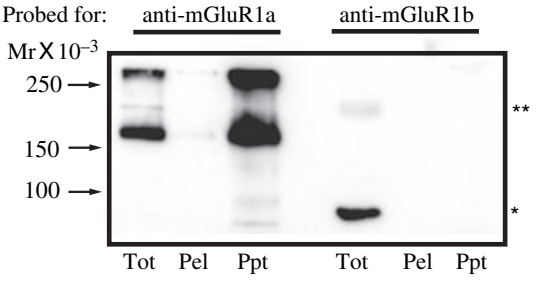

Fig. 4 Immunoprecipitation of mGluR1a from rat cerebellar membranes. The soluble material after a 100 000g_{av} centrifugation was immunoprecipitated for mGluR1a using an anti-mGluR1a C-terminal antibody, and the immunoprecipitate split into two aliquots before analysing the total lysate (Tot), the 100 000 g_{av} pellet (Pel) and the precipitate (Ppt) on a 5% SDS–polyacrylamide gel followed by immunoblotting for either mGluR1a or mGluR1b as indicated. Similar results were obtained in two separate experiments. The position of the molecular weight markers are indicated by the arrows and the position of the monomer and dimer forms of mGluR1b are indicated by the single and double asterisks respectively. Similar results were obtained in two separate experiments.

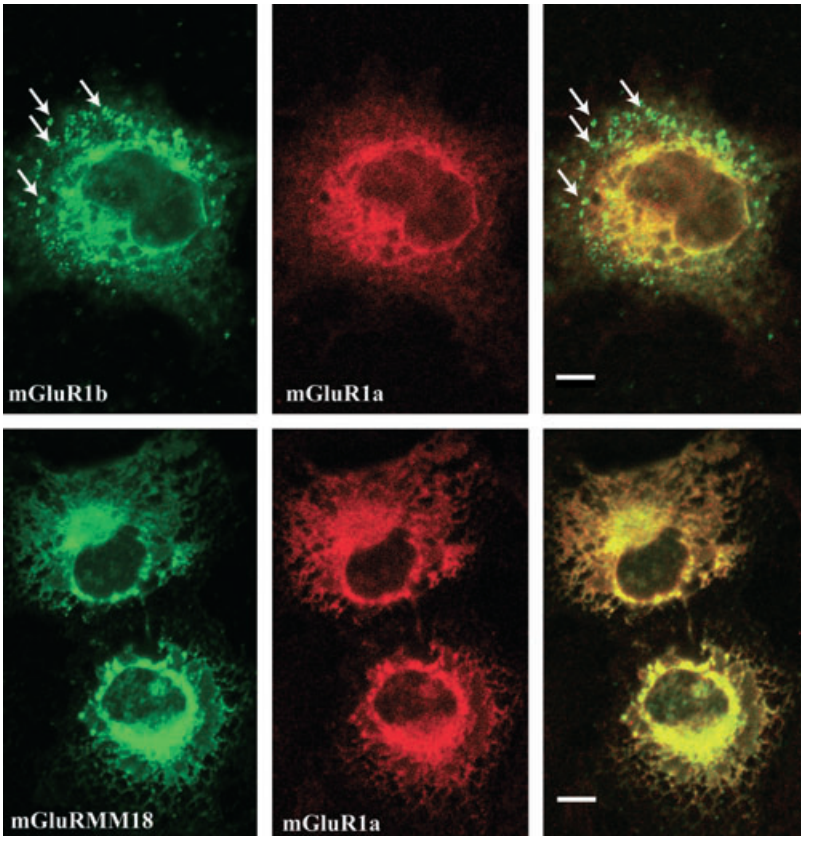

Fig. 5 Co-expression of mGluR1a with FLAG-tagged mGluR1b and co-expression of mGluR1a with FLAG-tagged mGluRMM18. COS-7 cells were transfected with the indicated constructs using a 1 : 1 ratio of DNA and 48 h later they were fixed, permeabilized and immunoreacted with an anti-FLAG antibody (mGluR1b and mGluRMM18) and with an anti-mGluR1a antibody (mGluR1a). The secondary antibodies were an Alexa 488-coupled goat anti-mouse antibody, and an Alexa 568-coupled goat anti-rabbit antibody. The scale bar represents (10 μm) and the right hand column shows the merged images of the red and green channels. The arrows indicate the intracellular accumulations formed by mGluR1b but not mGluRMM18.

demonstrate that mGluRMM18 and mGluR1a show an almost complete overlap in their intracellular distribution (Fig. 5 lower row), whereas mGluR1b, although clearly present in the ER with mGluR1a, gives multiple bright puncta of immunofluorescence that do not coincide with the immunostaining of mGluR1a (Fig. 5 upper row). This suggests that mGluR1b may be segregating from mGluR1a within the ER. To examine whether this behaviour of mGluR1b is conferred solely by the C-terminal tail, we made use of a reporter molecule, the lymphocyte surface antigen, CD2, where we replaced its C-terminus with that of mGluR1b to give pCD1b. This construct has been shown to convert CD2 from a fully glycosylated surface expressed protein into an ER retained EndoH sensitive form (Chan *et al.* 2001). We then co-expressed CD2-YFP with pCD1b in COS-7 cells, and following fixation and permeabilization, immunostained the cells for pCD1b with a C-terminal anti-mGluR1b antibody. CD2-YFP was clearly apparent at the cell surface (Fig. 6 upper row) whilst pCD1b was retained in the cells in large intracellular inclusions (Fig. 6 lower row). However where these inclusions were present, the fluorescence of CD2-YFP was significantly diminished suggesting that it was being excluded, at least in part, from these areas of the ER (Fig. 6 lower panel). Furthermore, the observation that CD2 was still being trafficked to the cell surface suggests that despite the formation of the pCD1b inclusions, the normal cell processing of membrane proteins was maintained. In order to see if the C-terminal tail of mGluR1b was allowing the CD2 to progress further than the ER we examined the localization of the pCD1b in different cell compartments. The results show that as before the large intracellular inclusions formed by pCD1b are immunoreactive with the ER marker PDI, but not with the Golgi marker GM130, or the exit site marker Sec 24 nor with the intermediate compartment marker ERGIC 53 (Fig. 7). Interestingly, neither the intracellular distribution of the latter two proteins appears to be altered despite the formation of the inclusions containing pCD1b (Fig. 7; left hand column, lower two rows). Thus, as suggested by the surface expression of CD2-YFP, the intracellular machinery for trafficking proteins to the cell membrane seems to continue to function despite the sequestration of pCD1b into the ER-derived inclusions.

Discussion

The use of the myc-His-tagged versions of mGluR1b and mGluR1MM18 in this study confirms and extends our previous finding that the RRKK motif in the C-terminus of mGluR1b retains the majority of the receptor in the ER (Chan *et al.* 2001). Despite this some receptor does arrive at the plasma membrane where it is functional, but this protein,

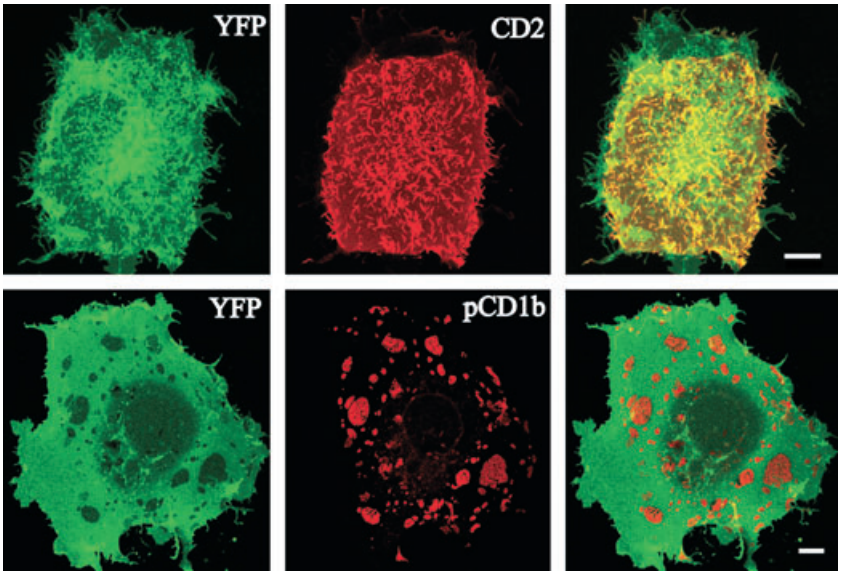

Fig. 6 COS-7 cells were transfected with the CD2-YFP and pCD1b constructs using a 1 : 1 ratio of DNA, and 48 h later they were fixed (upper panel) or fixed and permeabilized (lower panel). The cells in the upper panel were incubated with a mouse antibody to CD2 before being reacted with an Alexa 568-coupled anti mouse antibody to reveal the surface CD2. In the lower panel, the permeabilized cells were incubated with a rabbit anti-mGluR1b antibody before being reacted with an Alexa 568-coupled anti-rabbit antibody, to detect the intracellular pCD1b. The left hand column shows the YFP signal, the middle column shows the Alexa 568 signal and the right column panel shows the merged signals. The scale bar represents (10 μm).

previously quantified at 10% of the total, is EndoH sensitive, unlike mGluR1b found in the brain (Chan *et al.* 2001). Similar arginine-rich motifs have been described in other membrane proteins such as the NMDA receptor NR1 subunit (Standley *et al.* 2000), potassium channels (Zerangue *et al.* 1999), $GABA_B$ R1 (Margeta-Mitrovic 2002) and kainate receptors (Ren *et al.* 2003) and have been suggested to regulate the surface expression of these proteins. These studies have led to the suggestion that either RXR or ΦΨ/RRXR, where ΦΨ are any hydrophobic or aromatic amino acids and X is any amino acid, provide ER retention motifs at the appropriate place in the C-terminus of membrane proteins (Zerangue *et al.* 2001; Michelsen *et al.* 2005). The RRKK motif in mGluR1b does not conform to this consensus, and this may suggest that the domain in mGluR1b acts differently from other members of this type of ER retention motif.

Generally the ER retention of these proteins by the charged residues is overcome by the association of the retained protein with another receptor subunit as is the case for the $GABA_B$ receptor, potassium channels and NMDA receptor. In the latter case additional forward trafficking signals may involve the phosphorylation of residues flanking the retention motif and/or interaction with a PDZ-binding protein (Scott *et al.* 2001, 2003; Xia *et al.* 2001). Alternatively, the oligomerization of receptor subunits recruits additional proteins to facilitate the trafficking of the receptor, or channel complex, from the ER, as happens with the potassium channels and their recruitment of the 14-3-3 proteins after oligomerization (O'Kelly *et al.* 2002). One candidate for a partner protein to facilitate the trafficking of mGluR1b is mGluR1a, but as shown here it does not efficiently associate with mGluR1b in transiently transfected cells, or in the cerebellum. Consequently, in the brain where mGluR1b is fully glycosylated (Chan *et al.* 2001) there must exist other proteins that facilitate the trafficking of this receptor subtype, in this context it is interesting to note that a subunit of the $GABA_A$ receptor has been reported to promote the cell surface expression of $GABA_B$ R1 subunits (Balasubramanian *et al.* 2004).

The mechanism by which the arginine-based ER retention motifs operate is currently unclear, although clearly it causes the accumulation of mGluR1b in an ER-derived cell compartment. Indeed, the apparent sequestration of mGluR1b or a chimera of it into the ER-derived compartment may be one mechanism by which its dimerization with mGluR1a may be minimized. The ER accumulation of mGluR1b could result from its retrieval from the *cis*-Golgi apparatus or by its failure to utilize the normal trafficking mechanisms from the ER. This could reflect a failure of the receptor to interact with the coat protein 1or 2 complexes, respectively (Bonifacino and Lippincott-Schwartz 2003), and there is some evidence that at least some of the arginine-based motifs can bind coat protein 1 proteins (Yuan *et al.* 2003; Brock *et al.* 2005), although other studies suggest different mechanisms (Zerangue *et al.* 2001). As we could not detect the presence of mGluR1b or pCD1b in the Golgi apparatus, or in the ERGIC compartment it would seem that it is either actively retained in the ER or fails to leave it. In either case, its exit from the ER should involve either the formation, or the disruption, of a protein interaction. As the C-terminal tail of mGluR1b can act to restrict CD2 to the ER, it seems probable that this sequence of amino acids is sufficient to cause the ER retention. However, despite several attempts using the yeast two hybrid system and proteomic approaches, with both the normal mGluR1b C-terminus or that derived from mGluRMM18, we have so far failed to identify proteins interacting with this region of the receptor.

Our studies indicate that one function of the RRKK motif is to prevent the heterodimerization of mGluR1b with mGluR1a. Although using the more stringent solubilization

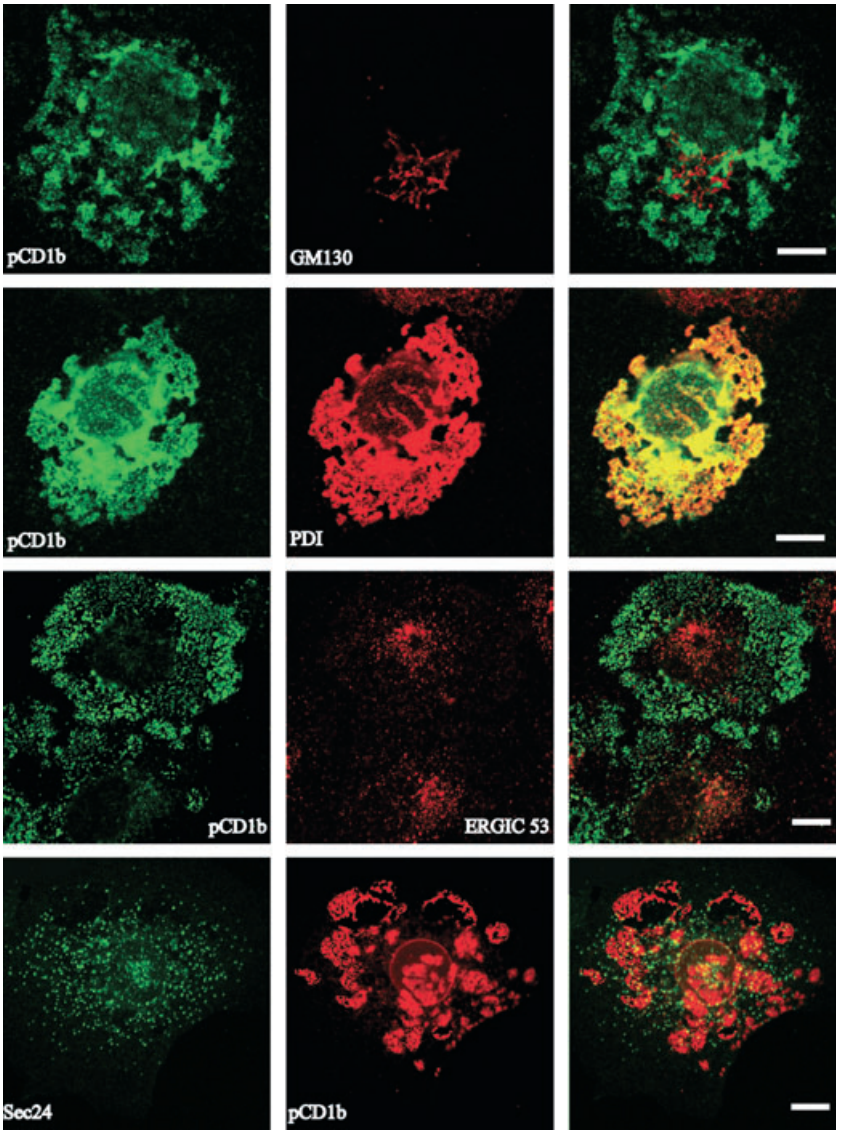

Fig. 7 Intracellular accumulations of pCD1b contain endoplasmic reticulum markers. COS-7 cells were transfected with pCD1b and 48 h later fixed using cold methanol and immunostained for pCD1b and the indicated marker proteins. pCD1b was detected using a rabbit anti-mGluR1b antibody in all the panels apart from the bottom row, where the mouse anti-CD2 was used. The secondary antibodies were an Alexa 568-coupled goat anti-mouse antibody, and an Alexa 488-coupled goat anti-rabbit antibody. The right hand column shows the merged images and the scale bar represents (10 μm).

conditions, permitted by the use of the Talon resin, to isolate potential heterodimers of mGluR1a and mGluR1b, did reveal occasional low levels of heterodimerization, these were much less than those found when the RRKK motif was removed by mutation. Likewise, no heterodimerization of these receptor subtypes was detected in rat cerebellum isolates, where both are expressed in the Purkinje cells. Interestingly, we were able to show clear homodimerization of both mGluR1b and mGluRMM18, but not heterodimerization of mGluR1b and mGluRMM18. This represents the first clear evidence that mGluR1b does exist as a homodimer and strongly suggests that the RRKK motif can regulate this dimerization.

As mGluR5a and mGluR5b, the other members of the mGluR Group 1 family, appear to heterodimerize efficiently and are well expressed at the cell surface, the question arises as to why the mGluR1 family has this RRKK motif that prevents heterodimerization of the receptor. In many cases, the heterodimerization between receptor subtypes, or even between different receptors, can result in a change of pharmacological properties [as observed for example for the opioid receptors (Jordan and Devi 1999) and taste receptors (Zhao *et al.* 2003)] or desensitization profile (as for the somatostatin receptor SSTR2/SSTR3 heterodimers; (Pfeiffer *et al.* 2001). As the functional differences between the two mGluR1 splice variants are minor (Pin *et al.* 1992; Joly *et al.* 1995; Mary *et al.* 1997) heterodimerization would not be expected to have a huge impact on the receptor properties. Nevertheless, heterodimerization would affect the array of proteins interacting with the dimeric mGluR. Thus mGluR1a, but not mGluR1b, can interact with the proteins Tamalin and Homer (Brakeman *et al.* 1997; Tu *et al.* 1998; Kitano *et al.* 2002). The interaction with Homer in particular can lead to association of mGluR1a with other proteins such as the IP_3 receptor and Shank (Tu *et al.* 1998, 1999). Indeed,

interaction of Homer and mGluR1a appears to modulate the constitutive activation of the receptor (Ango *et al.* 2001), and this and other Homer-mediated interactions can be modulated by the activity-induced expression of the dominant negative short variant Homer 1a (Minami *et al.* 2003). Therefore, the lack of heterodimerization between mGluR1a and mGluR1b keeps mGluR1b insensitive to the actions of Homer1a, creating a receptor pool with a functional profile similar to mGluR1a but differently regulated upon neuronal activation.

Acknowledgements

The authors would like to thank Dr David Stephens, Department of Biochemistry, Bristol University for the generous donation of an anti-Sec24 antibody and Professor Neil Barclay, William Dunn School of Pathology, Oxford for the gift of the plasmid for CD2 and the antibody OX34. RR was the recipient of a CASE studentship from the BBSRC and GlaxoSmithKline.

References

Ango F., Prezeau L., Muller T., Tu J. C., Xiao B., Worley P. F., Pin J. P., Bockaert J. and Fagni L. (2001) Agonist-independent activation of metabotropic glutamate receptors by the intracellular protein Homer. *Nature* **411**, 962–965.

Balasubramanian S., Teissere J. A., Raju D. V. and Hall R. A. (2004) Hetero-oligomerization between GABAA and GABAB receptors regulates GABAB receptor trafficking. *J. Biol. Chem.* **279**, 18840–18850.

Bessis A. S., Rondard P., Gaven F., Brabet I., Triballeau N., Prezeau L., Acher F. and Pin J. P. (2002) Closure of the Venus flytrap module of mGlu8 receptor and the activation process: insights from mutations converting antagonists into agonists. *Proc. Natl Acad. Sci. U. S. A.* **99**, 11097–11102.

Bonifacino J. S. and Lippincott-Schwartz J. (2003) Coat proteins: shaping membrane transport. *Nat. Rev. Mol. Cell Biol.* **4**, 409–414.

Brakeman P. R., Lanahan A. A., O'Brien R., Roche K., Barnes C. A., Huganir R. L. and Worley P. F. (1997) Homer: a protein that selectively binds metabotropic glutamate receptors. *Nature* **386**, 284–288.

Brock C., Boudier L., Maurel D., Blahos J. and Pin J. P. (2005) Assembly-dependent surface targeting of the heterodimeric GABAB receptor is controlled by COPI but not 14-3-3. *Mol. Biol. Cell* **16**, 5572–5578.

Chan W. Y., Soloviev M. M., Ciruela F. and McIlhinney R. A. J. (2001) Molecular determinants of metabotropic glutamate receptor 1B trafficking. *Mol. Cell. Neurosci.* **17**, 577–588.

Ciruela F., Soloviev M. M. and McIlhinney R. A. J. (1999a) Co-expression of metabotropic glutamate receptor type 1 alpha with Homer-1a/Vesl-1S increases the cell surface expression of the receptor. *Biochem. J.* **341**, 795–803.

Ciruela F., Soloviev M. M. and McIlhinney R. A. J. (1999b) Cell surface expression of the metabotropic glutamate receptor type 1α is regulated by the C-terminal tail. *FEBS Lett.* **448**, 91–94.

Ciruela F., Soloviev M. M., Chan W. Y. and McIlhinney R. A. J. (2000) Homer-1c/Vesl-1L modulates the cell surface targeting of metabotropic glutamate receptor type 1 alpha: evidence for an anchoring function. *Mol. Cell. Neurosci.* **15**, 36–50.

Conn P. J. and Pin J. P. (1997) Pharmacology and functions of metabotropic glutamate receptors. *Ann. Rev. Pharmacol. Toxicol.* **37**, 205–237.

Francesconi A. and Duvoisin R. M. (2002) Alternative splicing unmasks dendritic and axonal targeting signals in metabotropic glutamate receptor 1. *J. Neurosci.* **22**, 2196–2205.

Gama L., Wilt S. G. and Breitwieser G. E. (2001) Heterodimerization of calcium sensing receptors with metabotropic glutamate receptors in neurons. *J. Biol. Chem.* **276**, 39053–39059.

Han G. and Hampson D. R. (1999) Ligand binding to the amino-terminal domain of the mGluR4 subtype of metabotropic glutamate receptor. *J. Biol. Chem.* **274**, 10008–10013.

Hollmann M. and Heinemann S. (1994) Cloned glutamate receptors. *Annu. Rev. Neurosci.* **17**, 31–108.

Joly C., Gomeza J., Brabet I., Curry K., Bockaert J. and Pin J. P. (1995) Molecular, functional, and pharmacological characterization of the metabotropic glutamate receptor type 5 splice variants: comparison with mGluR1. *J. Neurosci.* **15**, 3970–3981.

Jordan B. A. and Devi L. A. (1999) G-protein heterodimerization modulates receptor function. *Nature* **399**, 697–700.

Jordan M., Schallhorn A. and Wurm F. M. (1996) Transfecting mammalian cells: optimization of critical parameters affecting calcium phosphate precipitate formation. *Nucleic Acids Res.* **24**, 596–601.

Kitano J., Kimura K., Yamazaki Y., Soda T., Shigemoto R., Nakajima Y. and Nakanishi S. (2002) Tamalin, a PDZ domain-containing protein, links a protein complex formation of group 1 metabotropic glutamate receptors and the guanine nucleotide exchange factor cytohesins. *J. Neurosci.* **22**, 1280–1289.

Kniazeff J., Bessis A. S., Maurel D., Ansanay H., Prezeau L. and Pin J. P. (2004a) Closed state of both binding domains of homodimeric mGlu receptors is required for full activity. *Nat. Struct. Mol. Biol.* **11**, 706–713.

Kniazeff J., Saintot P. P., Goudet C., Liu J., Charnet A., Guillon G. and Pin J. P. (2004b) Locking the dimeric GABA(B) G-protein-coupled receptor in its active state. *J. Neurosci.* **24**, 370–377.

Kunishima N., Shimada Y., Tsuji Y., Sato T., Yamamoto M., Kumasaka T., Nakanishi S., Jingami H. and Morikawa K. (2000) Structural basis of glutamate recognition by a dimeric metabotropic glutamate receptor. *Nature* **407**, 971–977.

Liu J., Maurel D., Etzol S., Brabet I., Ansanay H., Pin J. P. and Rondard P. (2004a) Molecular determinants involved in the allosteric control of agonist affinity in the GABAB receptor by the GABAB2 subunit. *J. Biol. Chem.* **279**, 15824–15830.

Liu J., Ernst S. A., Gladycheva S. E., Lee Y. Y., Lentz S. I., Ho C. S., Li Q. and Stuenkel E. L. (2004b) Fluorescence resonance energy transfer reports properties of syntaxin1a interaction with Munc18-1 in vivo. *J. Biol. Chem.* **279**, 55924–55936.

Malenka R. C. and Nicoll R. A. (1993) NMDA-receptor-dependent synaptic plasticity: multiple forms and mechanisms. *Trends Neurosci.* **16**, 521–527.

Margeta-Mitrovic M. (2002) Assembly-dependent trafficking assays in the detection of receptor-receptor interactions. *Methods* **27**, 311–317.

Mary S., Stephan D., Gomeza J., Bockaert J., Pruss R. M. and Pin J. P. (1997) The rat mGlu1d receptor splice variant shares functional properties with the other short isoforms of mGlu1 receptor. *Eur. J. Pharmacol.* **335**, 65–72.

Mary S., Gomeza J., Prezeau L., Bockaert J. and Pin J. P. (1998) A cluster of basic residues in the carboxyl-terminal tail of the short metabotropic glutamate receptor 1 variants impairs their coupling to phospholipase C. *J. Biol. Chem.* **273**, 425–432.

Mateos J. M., Azkue J., Benitez R., Sarria R., Losada J., Conquet F., Ferraguti F., Kuhn R., Knopfel T. and Grandes P. (1998) Immunocytochemical localization of the mGluR1b metabotropic glutamate receptor in the rat hypothalamus. *J. Comp. Neurol.* **390**, 225–233.

Mateos J. M., Benitez R., Elezgarai I. *et al.* (2000) Immunolocalization of the mGluR1b splice variant of the metabotropic glutamate receptor 1 at parallel fiber-Purkinje cell synapses in the rat cerebellar cortex. *J. Neurochem.* **74**, 1301–1309.

Mayer M. L. and Westbrook G. L. (1987) The physiology of excitatory amino acids in the vertebrate central nervous system. *Prog. Neurobiol.* **28**, 197–276.

Michelsen K., Yuan H. and Schwappach B. (2005) Hide and run. Arginine-based endoplasmic-reticulum-sorting motifs in the assembly of heteromultimeric membrane proteins. *EMBO Rep* **6**, 717–722.

Minami I., Kengaku M., Smitt P. S., Shigemoto R. and Hirano T. (2003) Long-term potentiation of mGluR1 activity by depolarization-induced Homer1a in mouse cerebellar Purkinje neurons. *Eur. J. Neurosci.* **17**, 1023–1032.

Mion S., Corti C., Neki A., Shigemoto R., Corsi M., Fumagalli G. and Ferraguti F. (2001) Bidirectional regulation of neurite elaboration by alternatively spliced metabotropic glutamate receptor 5 (mGluR5) isoforms. *Mol. Cell. Neurosci.* **17**, 957–972.

Nashmi R., Dickinson M. E., McKinney S., Jareb M., Labarca C., Fraser S. E. and Lester H. A. (2003) Assembly of alpha4beta2 nicotinic acetylcholine receptors assessed with functional fluorescently labeled subunits: effects of localization, trafficking, and nicotine-induced upregulation in clonal mammalian cells and in cultured midbrain neurons. *J. Neurosci.* **23**, 11554–11567.

O'Kelly I., Butler M. H., Zilberberg N. and Goldstein S. A. (2002) Forward transport. 14-3-3 binding overcomes retention in endoplasmic reticulum by dibasic signals. *Cell* **111**, 577–588.

Pfeiffer M., Koch T., Schroder H., Klutzny M., Kirscht S., Kreienkamp H. J., Hollt V. and Schulz S. (2001) Homo- and heterodimerization of somatostatin receptor subtypes. Inactivation of sst(3) receptor function by heterodimerization with sst(2A). *J. Biol. Chem.* **276**, 14027–14036.

Pin J. P. and Acher F. (2002) The metabotropic glutamate receptors: structure, activation mechanism and pharmacology. *Curr. Drug Targets CNS Neurol. Disord.* **1**, 297–317.

Pin J. P. and Duvoisin R. (1995) The metabotropic glutamate receptors: structure and functions. *Neuropharmacology* **34**, 1–26.

Pin J. P., Waeber C., Prezeau L., Bockaert J. and Heinemann S. F. (1992) Alternative splicing generates metabotropic glutamate receptors inducing different patterns of calcium release in *Xenopus* oocytes. *Proc. Natl Acad. Sci. USA* **89**, 10331–10335.

Pin J. P., Kniazeff J., Goudet C., Bessis A. S., Liu J., Galvez T., Acher F., Rondard P. and Prezeau L. (2004) The activation mechanism of class-C G-protein coupled receptors. *Biol. Cell* **96**, 335–342.

Ray K. and Hauschild B. C. (2000) Cys-140 is critical for metabotropic glutamate receptor-1 dimerization. *J. Biol. Chem.* **275**, 34245–34251.

Ray K., Hauschild B. C., Steinbach P. J., Goldsmith P. K., Hauache O. and Spiegel A. M. (1999) Identification of the cysteine residues in the amino-terminal extracellular domain of the human Ca(2+) receptor critical for dimerization. Implications for function of monomeric Ca(2+) receptor. *J. Biol. Chem.* **274**, 27642–27650.

Ren Z., Riley N. J., Needleman L. A., Sanders J. M., Swanson G. T. and Marshall J. (2003) Cell surface expression of GluR5 kainate receptors is regulated by an endoplasmic reticulum retention signal. *J. Biol. Chem.* **278**, 52700–52709.

Robbins M. J., Ciruela F., Rhodes A. and McIlhinney R. A. (1999) Characterization of the dimerization of metabotropic glutamate receptors using an N-terminal truncation of mGluR1alpha. *J. Neurochem.* **72**, 2539–2547.

Robbins M. J., Michalovich D., Hill J., Calver A. R., Medhurst A. D., Gloger I., Sims M., Middlemiss D. N. and Pangalos M. N. (2000) Molecular cloning and characterization of two novel retinoic acid-inducible orphan G-protein-coupled receptors (GPRC5B and GPRC5C). *Genomics* **67**, 8–18.

Romano C., Yang W. L. and Omalley K. L. (1996) Metabotropic glutamate receptor 5 is a disulfide-linked dimer. *J. Biol. Chem.* **271**, 28612–28616.

Romano C., Miller J. K., Hyrc K., Dikranian S., Mennerick S., Takeuchi Y., Goldberg M. P. and OMalley K. L. (2001) Covalent and non-covalent interactions mediate metabotropic glutamate receptor mGlu(5) dimerization. *Mol. Pharmacol.* **59**, 46–53.

Scott D. B., Blanpied T. A., Swanson G. T., Zhang C. F. and Ehlers M. D. (2001) An NMDA receptor ER retention signal regulated by phosphorylation and. *J. Neurosci.* **21**, 3063–3072.

Scott D. B., Blanpied T. A. and Ehlers M. D. (2003) Coordinated PKA and PKC phosphorylation suppresses RXR-mediated ER retention and regulates the surface delivery of NMDA receptors. *Neuropharmacology* **45**, 755–767.

Selkirk J. V., Challiss R. A., Rhodes A. and McIlhinney R. A. (2002) Characterization of an N-terminal secreted domain of the type-1 human metabotropic glutamate receptor produced by a mammalian cell line. *J. Neurochem.* **80**, 346–353.

Standley S., Roche K. W., McCallum J., Sans N. and Wenthold R. J. (2000) PDZ domain suppression of an ER retention signal in NMDA receptor NR1 splice variants. *Neuron* **28**, 887–898.

Tanabe Y., Masu M., Ishii T., Shigemoto S. and Nakanishi S. (1992) A family of metabotropic glutamate receptors. *Neuron* **8**, 169–179.

Tateyama M., Abe H., Nakata H., Saito O. and Kubo Y. (2004) Ligand-induced rearrangement of the dimeric metabotropic glutamate receptor 1alpha. *Nat. Struct. Mol. Biol.* **11**, 637–642.

Tsuchiya D., Kunishima N., Kamiya N., Jingami H. and Morikawa K. (2002) Structural views of the ligand-binding cores of a metabotropic glutamate receptor complexed with an antagonist and both glutamate and Gd3+. *Proc. Natl Acad. Sci. USA* **99**, 2660–2665.

Tsuji Y., Shimada Y., Takeshita T., Kajimura N., Nomura S., Sekiyama N., Otomo J., Usukura J., Nakanishi S. and Jingami H. (2000) Cryptic dimer interface and domain organization of the extracellular region of metabotropic glutamate receptor subtype 1. *J. Biol. Chem.* **275**, 28144–28151.

Tu J. C., Xiao B., Yuan J. P., Lanahan A. A., Leoffert K., Li M., Linden D. J. and Worley P. F. (1998) Homer binds a novel proline rich motif and links group 1 metabotropic glutamate receptors with IP3 receptors. *Neuron* **21**, 717–726.

Tu J. C., Xiao B., Naisbitt S. *et al.* (1999) Coupling of mGluR/Homer and PSD-95 complexes by the Shank family of postsynaptic density proteins. *Neuron* **23**, 583–592.

Villemure J. F., Adam L., Bevan N. J., Gearing K., Chenier S. and Bouvier M. (2005) Subcellular distribution of GABA(B) receptor homo- and hetero-dimers. *Biochem. J.* **388**, 47–55.

Xia H., Hornby Z. D. and Malenka R. C. (2001) An ER retention signal explains differences in surface expression of NMDA and AMPA receptor subunits. *Neuropharmacology* **41**, 714–723.

Yuan H., Michelsen K. and Schwappach B. (2003) 14-3-3 dimers probe the assembly status of multimeric membrane proteins. *Curr. Biol.* **13**, 638–646.

Zerangue N., Schwappach B., Jan Y. N. and Jan L. Y. (1999) A new ER trafficking signal regulates the subunit stoichiometry of plasma membrane K_{ATP} channels. *Neuron* **22**, 537–548.

Zerangue N., Malan M. J., Fried S. R., Dazin P. F., Jan Y. N., Jan L. Y. and Schwappach B. (2001) Analysis of endoplasmic reticulum trafficking signals by combinatorial screening in mammalian cells. *Proc. Natl Acad. Sci. USA* **98**, 2431–2436.

Zhao G. Q., Zhang Y., Hoon M. A., Chandrashekar J., Erlenbach I., Ryba N. J. and Zuker C. S. (2003) The receptors for mammalian sweet and umami taste. *Cell* **115**, 255–266.

